

Search for correlations between arrival directions of ultrahigh-energy cosmic rays detected by the Telescope Array experiment and a flux pattern from nearby starburst galaxies

TELESCOPE ARRAY COLLABORATION

R.U. ABBASI,¹ M. ABE,² T. ABU-ZAYYAD,¹ M. ALLEN,¹ R. AZUMA,³ E. BARCIKOWSKI,¹ J.W. BELZ,¹ D.R. BERGMAN,¹ S.A. BLAKE,¹ R. CADY,¹ B.G. CHEON,⁴ J. CHIBA,⁵ M. CHIKAWA,⁶ A. DI MATTEO,⁷ T. FUJII,⁸ K. FUJITA,⁹ M. FUKUSHIMA,^{8,10} G. FURLICH,¹ T. GOTO,⁹ W. HANLON,¹ M. HAYASHI,¹¹ Y. HAYASHI,⁹ N. HAYASHIDA,¹² K. HIBINO,¹³ K. HONDA,¹³ D. IKEDA,⁸ N. INOUE,² T. ISHII,¹³ R. ISHIMORI,³ H. ITO,¹⁴ D. IVANOV,¹ H.M. JEONG,¹⁵ S. JEONG,¹⁵ C.C.H. JUI,¹ K. KADOTA,¹⁶ F. KAKIMOTO,³ O. KALASHEV,¹⁷ K. KASAHARA,¹⁸ H. KAWAI,¹⁹ S. KAWAKAMI,⁹ S. KAWANA,² K. KAWATA,⁸ E. KIDO,⁸ H.B. KIM,⁴ J.H. KIM,⁴ J.H. KIM,²⁰ S. KISHIGAMI,⁹ S. KITAMURA,³ Y. KITAMURA,³ V. KUZMIN,^{17,*} M. KUZNETSOV,¹⁷ Y.J. KWON,²¹ K.H. LEE,¹⁵ B. LUBSANDORZHIEV,¹⁷ J.P. LUNDQUIST,¹ K. MACHIDA,¹³ K. MARTENS,¹⁰ T. MATSUYAMA,⁹ J.N. MATTHEWS,¹ R. MAYTA,⁹ M. MINAMINO,⁹ K. MUKAI,¹³ I. MYERS,¹ K. NAGASAWA,² S. NAGATAKI,¹⁴ R. NAKAMURA,²² T. NAKAMURA,²³ T. NONAKA,⁸ H. ODA,⁹ S. OGIO,⁹ J. OGURA,³ M. OHNISHI,⁸ H. OHOKA,⁸ T. OKUDA,²⁴ Y. OMURA,⁹ M. ONO,¹⁴ R. ONOGI,⁹ A. OSHIMA,⁹ S. OZAWA,¹⁸ I.H. PARK,¹⁵ M.S. PSHIRKOV,^{17,25} J. REMINGTON,¹ D.C. RODRIGUEZ,¹ G. RUBTSOV,¹⁷ D. RYU,²⁰ H. SAGAWA,⁸ R. SAHARA,⁹ K. SAITO,⁸ Y. SAITO,²² N. SAKAKI,⁸ N. SAKURAI,⁹ L.M. SCOTT,²⁶ T. SEKI,²² K. SEKINO,⁸ P.D. SHAH,¹ F. SHIBATA,¹³ T. SHIBATA,⁸ H. SHIMODAIRA,⁸ B.K. SHIN,⁹ H.S. SHIN,⁸ J.D. SMITH,¹ P. SOKOLSKY,¹ B.T. STOKES,¹ S.R. STRATTON,^{1,26} T.A. STROMAN,¹ T. SUZAWA,² Y. TAKAGI,⁹ Y. TAKAHASHI,⁹ M. TAKAMURA,⁵ M. TAKEDA,⁸ R. TAKEISHI,¹⁵ A. TAKETA,²⁷ M. TAKITA,⁸ Y. TAMEDA,²⁸ H. TANAKA,⁹ K. TANAKA,²⁹ M. TANAKA,³⁰ S.B. THOMAS,¹ G.B. THOMSON,¹ P. TINYAKOV,^{17,7} I. TKACHEV,¹⁷ H. TOKUNO,³ T. TOMIDA,²² S. TROITSKY,¹⁷ Y. TSUNESADA,⁹ K. TSUTSUMI,³ Y. UCHIHORI,³¹ S. UDO,¹² F. URBAN,³² T. WONG,¹ M. YAMAMOTO,²² R. YAMANE,⁹ H. YAMAOKA,³⁰ K. YAMAZAKI,¹² J. YANG,³³ K. YASHIRO,⁵ Y. YONEDA,⁹ S. YOSHIDA,¹⁹ H. YOSHII,³⁴ Y. ZHEZHER,¹⁷ AND Z. ZUNDEL¹

¹High Energy Astrophysics Institute and Department of Physics and Astronomy, University of Utah, Salt Lake City, Utah, USA

²The Graduate School of Science and Engineering, Saitama University, Saitama, Saitama, Japan

³Graduate School of Science and Engineering, Tokyo Institute of Technology, Meguro, Tokyo, Japan

⁴Department of Physics and The Research Institute of Natural Science, Hanyang University, Seongdong-gu, Seoul, Korea

⁵Department of Physics, Tokyo University of Science, Noda, Chiba, Japan

⁶Department of Physics, Kindai University, Higashi Osaka, Osaka, Japan

⁷Service de Physique Thorique, Universit Libre de Bruxelles, Brussels, Belgium

⁸Institute for Cosmic Ray Research, University of Tokyo, Kashiwa, Chiba, Japan

⁹Graduate School of Science, Osaka City University, Osaka, Osaka, Japan

¹⁰Kavli Institute for the Physics and Mathematics of the Universe (WPI), Todai Institutes for Advanced Study, University of Tokyo, Kashiwa, Chiba, Japan

¹¹Information Engineering Graduate School of Science and Technology, Shinshu University, Nagano, Nagano, Japan

¹²Faculty of Engineering, Kanagawa University, Yokohama, Kanagawa, Japan

¹³Interdisciplinary Graduate School of Medicine and Engineering, University of Yamanashi, Kofu, Yamanashi, Japan

¹⁴Astrophysical Big Bang Laboratory, RIKEN, Wako, Saitama, Japan

¹⁵Department of Physics, Sungkyunkwan University, Jang-an-gu, Suwon, Korea

¹⁶Department of Physics, Tokyo City University, Setagaya-ku, Tokyo, Japan

¹⁷Institute for Nuclear Research of the Russian Academy of Sciences, Moscow, Russia

¹⁸Advanced Research Institute for Science and Engineering, Waseda University, Shinjuku-ku, Tokyo, Japan

¹⁹Department of Physics, Chiba University, Chiba, Chiba, Japan

²⁰Department of Physics, School of Natural Sciences, Ulsan National Institute of Science and Technology, UNIST-gil, Ulsan, Korea

²¹Department of Physics, Yonsei University, Seodaemun-gu, Seoul, Korea

²²Academic Assembly School of Science and Technology Institute of Engineering, Shinshu University, Nagano, Nagano, Japan

²³Faculty of Science, Kochi University, Kochi, Kochi, Japan

²⁴Department of Physical Sciences, Ritsumeikan University, Kusatsu, Shiga, Japan

²⁵Sternberg Astronomical Institute, Moscow M.V. Lomonosov State University, Moscow, Russia

²⁶Department of Physics and Astronomy, Rutgers University - The State University of New Jersey, Piscataway, New Jersey, USA

²⁷Earthquake Research Institute, University of Tokyo, Bunkyo-ku, Tokyo, Japan

²⁸*Department of Engineering Science, Faculty of Engineering, Osaka Electro-Communication University, Neyagawa-shi, Osaka, Japan*

²⁹*Graduate School of Information Sciences, Hiroshima City University, Hiroshima, Hiroshima, Japan*

³⁰*Institute of Particle and Nuclear Studies, KEK, Tsukuba, Ibaraki, Japan*

³¹*National Institute of Radiological Science, Chiba, Chiba, Japan*

³²*CEICO, Institute of Physics, Czech Academy of Sciences, Prague, Czech Republic*

³³*Department of Physics and Institute for the Early Universe, Ewha Womans University, Seodaemun-gu, Seoul, Korea*

³⁴*Department of Physics, Ehime University, Matsuyama, Ehime, Japan*

(Received September 3, 2022)

Submitted to ApJL

ABSTRACT

The Pierre Auger Collaboration (Auger) recently reported a correlation between the arrival directions of cosmic rays with energies above 39 EeV and the flux pattern of 23 nearby starburst galaxies (SBGs). In this Letter, we tested the same hypothesis using cosmic rays detected by the Telescope Array experiment (TA) in the 9-year period from May 2008 to May 2017. Unlike the Auger analysis, we did not optimize the parameter values but kept them fixed to the best-fit values found by Auger, namely 9.7% for the anisotropic fraction of cosmic rays assumed to originate from the SBGs in the list and 12.9° for the angular scale of the correlations. The energy threshold we adopted is 43 EeV, corresponding to 39 EeV in Auger when taking into account the energy-scale difference between two experiments. We find that the TA data is compatible with isotropy to within 1.2σ and with the Auger result to within 1.3σ .

Keywords: astroparticle physics — cosmic rays — galaxies: starburst — methods: data analysis

1. INTRODUCTION

The origins of ultrahigh-energy cosmic rays (UHECRs) are still unknown. Anisotropies in the angular distribution of their arrival directions are rather small, requiring the detection of a large number of events to observe them. Furthermore, deflections of UHECRs by Galactic and intergalactic magnetic fields complicate the interpretation of anisotropies in terms of possible sources; this effect is reduced for the highest-energy cosmic rays, but the available statistics are significantly limited due to the steeply falling spectrum of UHECRs.

The two largest UHECR observatories in operation are the Telescope Array (hereinafter TA, [Abu-Zayyad et al. 2013a](#)), located in Utah, USA, with approximately 700 km^2 effective area, and the Pierre Auger Observatory (hereinafter Auger, [Aab et al. 2015](#)), located in Argentina with 3000 km^2 effective area. Their exposures peak in the Northern and Southern hemispheres, respectively.

Auger recently reported ([Aab et al. 2018](#)) a correlation between UHECR events with reconstructed energies above 39 EeV and a flux pattern of nearby starburst galaxies (SBGs). A model where 90.3% of the flux is isotropic and 9.7% originates from SBGs (with UHECR

luminosities assumed proportional to their radio luminosities) and undergoes Gaussian random deflections with standard deviation 12.9° in each transverse dimension is favored over the purely isotropic model with a post-trial significance of 4.0σ , and over a model based on the overall galaxy distribution beyond 1 Mpc with a 3.0σ significance. In the Auger analysis it was found that different selections of candidate sources yield very similar results, as in any case over 90% of the anisotropic part of the flux weighed by the Auger directional exposure originates from four bright objects — NGC 4945, NGC 253, M83, and NGC 1068.

In this Letter, we follow up on this finding by testing UHECRs detected by TA in the Northern hemisphere against the same flux model and the best-fit values reported by Auger, and discuss possible interpretations of our result.

2. ANALYSIS

2.1. Cosmic-ray dataset

The TA is located at 39.3° N , 112.9° W , in Millard County, Utah, USA, about 200 km south-west of Salt Lake City, about 1400 m above sea level ([Abu-Zayyad et al. 2013a](#)). The TA surface detector (SD) array consists of 507 plastic scintillation detectors on a square grid with 1.2 km spacing, covering an area of 700 km^2 , and is surrounded by three fluorescence detector (FD) stations

* Deceased

(Tokuno et al. 2012) with telescopes overlooking the SD array. It has been collecting data since May 2008. The SD has $\approx 100\%$ duty cycle, against $\approx 10\%$ for the FD, so with a similar collection area the SD has about ten times the statistics. The events detected in coincidence by both detectors are used to calibrate energy scale of the SD: SD reconstructed energies (determined by comparison to Monte Carlo simulations) are rescaled by a factor of $1/1.27$ to match the FD energy scale (determined calorimetrically) (Abu-Zayyad et al. 2013b; Tsunesada et al. 2017). The systematic uncertainty on the TA energy scale is 21% (Abbasi et al. 2016) and its energy and angular resolutions are 15–20% and 1.0–1.5°, respectively, depending on the event geometry and energy (Abbasi et al. 2014).

In this work we use data collected by the TA SD array in a 9-year period from May 2008 to May 2017 with reconstructed energies above 43 EeV and zenith angles less than 55°, using the same quality cuts as in Abbasi et al. (2014). This dataset comprises 284 events. We neglect the finite angular and energy resolution of TA events, and consider the detector fully efficient, i.e. with a flat response for all showers with energies and zenith angles in the considered range, so that its directional exposure ω_{TA} equals the geometrical one, which varies with declination δ but not with right ascension α (Somers 2001):

$$\omega_{\text{TA}}(\delta) \propto \cos \phi_{\text{TA}} \cos \delta \sin \alpha_{\text{m}} + \alpha_{\text{m}} \sin \phi_{\text{TA}} \sin \delta, \quad (1)$$

$$\alpha_{\text{m}} = \begin{cases} \pi, & \xi < -1; \\ \arccos \xi, & -1 \leq \xi \leq 1; \\ 0, & \xi > 1; \end{cases}$$

$$\xi = \frac{\cos \theta_{\text{m}} - \sin \phi_{\text{TA}} \sin \delta}{\cos \phi_{\text{TA}} \cos \delta},$$

where $\phi_{\text{TA}} = +39.3^\circ$ is the detector latitude and $\theta_{\text{m}} = 55^\circ$ is the maximum zenith angle accepted.

The energy threshold of $E_{\text{min}} = 43$ EeV used in this analysis corresponds to the Auger energy threshold of 39 EeV at which the most significant correlation with SBG was found. Here we took into account the 10.4% difference between the energy scales of the two experiments as estimated by a comparison of energy spectra around 5 EeV (AbuZayyad et al. 2018; Verzi et al. 2017).

2.2. Source catalog

Following the Auger analysis (Aab et al. 2018), we select the candidate sources from a sample of 63 SBGs outside the Local Group compiled by the *Fermi*-LAT collaboration (Ackermann et al. 2012) for the gamma-ray

Table 1. Selected source candidates from the SBG catalog used in this analysis (the same as in Aab et al. 2018). The last column shows the relative source contribution weighted with the TA directional exposure ω_{TA} .

name	Gal. (l, b)	distance	flux ϕ	$\phi\omega_{\text{TA}}$
NGC 253	97.4° −88.0°	2.7 Mpc	13.6%	1.6%
M82	141.4° 40.6°	3.6 Mpc	18.6%	35.7%
NGC 4945	305.3° 13.3°	4.0 Mpc	16.0%	0.0%
M83	314.6° 32.0°	4.0 Mpc	6.3%	0.4%
IC 342	138.2° 10.6°	4.0 Mpc	5.5%	10.5%
NGC 6946	95.7° 11.7°	5.9 Mpc	3.4%	6.2%
NGC 2903	208.7° 44.5°	6.6 Mpc	1.1%	1.4%
NGC 5055	106.0° 74.3°	7.8 Mpc	0.9%	1.5%
NGC 3628	240.9° 64.8°	8.1 Mpc	1.3%	1.5%
NGC 3627	242.0° 64.4°	8.1 Mpc	1.1%	1.2%
NGC 4631	142.8° 84.2°	8.7 Mpc	2.9%	4.4%
M51	104.9° 68.6°	10.3 Mpc	3.6%	6.2%
NGC 891	140.4° −17.4°	11.0 Mpc	1.7%	2.8%
NGC 3556	148.3° 56.3°	11.4 Mpc	0.7%	1.3%
NGC 660	141.6° −47.4°	15.0 Mpc	0.9%	1.0%
NGC 2146	135.7° 24.9°	16.3 Mpc	2.6%	5.2%
NGC 3079	157.8° 48.4°	17.4 Mpc	2.1%	3.8%
NGC 1068	172.1° −51.9°	17.9 Mpc	12.1%	9.1%
NGC 1365	238.0° −54.6°	22.3 Mpc	1.3%	0.0%
Arp 299	141.9° 55.4°	46.0 Mpc	1.6%	2.9%
Arp 220	36.6° 53.0°	80.0 Mpc	0.8%	1.1%
NGC 6240	20.7° 27.3°	105.0 Mpc	1.0%	0.8%
Mkn 231	121.6° 60.2°	183.0 Mpc	0.8%	1.4%

emission search.¹ Imposing the cut of flux greater than 0.3 Jy at 1.4 GHz leaves 23 objects in the catalog of candidate sources. Their UHECR fluxes were assumed to be proportional to their radio fluxes at 1.4 GHz. These objects are listed in Table 1.

In the Auger analysis, the effect of energy losses by UHECRs during their propagation was found to be negligible in the SBG model, as most of the anisotropic flux originates from sources within a few Mpc; in this work, we neglected the losses for simplicity.

2.3. Test statistic and flux model

Let $\hat{\mathbf{n}}$ be the unit vector representing a direction in the sky, pointing away from the observer. Given two flux models $\Phi_1(\hat{\mathbf{n}})$, $\Phi_2(\hat{\mathbf{n}})$ describing a null hypothesis and an alternative hypothesis, respectively, and the directional exposure $\omega(\hat{\mathbf{n}})$ of an experiment, the test statistic (here-

¹ Only four of those objects were actually successfully detected in gamma rays in that work: NGC 253, M82, NGC 4945 and NGC 1068.

inafter TS) is defined as twice the log-likelihood ratio

$$\text{TS} = 2 \ln(L(\Phi_2)/L(\Phi_1)), \quad (2)$$

$$\text{where } L(\Phi_j) = \prod_i \frac{\Phi_j(\hat{\mathbf{n}}_i)\omega(\hat{\mathbf{n}}_i)}{\int_{4\pi} \Phi_j(\hat{\mathbf{n}})\omega(\hat{\mathbf{n}}) d\Omega},$$

and $\hat{\mathbf{n}}_i$ being the reconstructed arrival direction of the i -th observed event. A positive (negative) TS indicates that the dataset is more (less) likely if the real flux is described by $\Phi_2(\hat{\mathbf{n}})$ than by $\Phi_1(\hat{\mathbf{n}})$.

In this analysis, the null hypothesis is an isotropic flux, $\Phi_1(\hat{\mathbf{n}}) = \Phi_{\text{iso}} = 1/4\pi$, whereas the alternative hypothesis is $\Phi_2(\hat{\mathbf{n}}) =$

$$\Phi_{\text{mod}}(\hat{\mathbf{n}}) = f_{\text{SBG}}\Phi_{\text{SBG}}(\hat{\mathbf{n}}) + (1 - f_{\text{SBG}})\Phi_{\text{iso}}, \quad (3)$$

where $f_{\text{SBG}} = 9.7\%$ is the fraction of the flux assumed to originate from the SBGs in the catalog (the rest being assumed to be isotropic), and

$$\Phi_{\text{SBG}}(\hat{\mathbf{n}}) = \frac{\sum_k \phi_k \exp(\hat{\mathbf{n}}_k \cdot \hat{\mathbf{n}}/\theta^2)}{\int_{4\pi} \sum_k \phi_k \exp(\hat{\mathbf{n}}_k \cdot \hat{\mathbf{n}}/\theta^2) d\Omega} \quad (4)$$

is a weighed sum of von Mises–Fisher distributions (the spherical analog of the Gaussian distribution), where ϕ_k and $\hat{\mathbf{n}}_k$ are the flux and position of the k -th source from Table 1 and $\theta = 12.9^\circ$ is the RMS deviation in each transverse dimension, the total RMS deviation being $\sqrt{2}\theta$. The exposure is assumed to be geometrical, $\omega(\hat{\mathbf{n}}) = \omega_{\text{TA}}(\hat{\mathbf{n}})$ from eq. (1). In the present work we do not optimize the parameter values but keep them fixed to the Auger best-fit values, in order not to include any freedom in the model which would require a statistical penalty. The resulting model flux is shown in Figure 1, along with the events in the TA dataset.

3. RESULTS

Substituting the coordinates of the TA events $\{\hat{\mathbf{n}}_i\}$ into equation (2), the test statistic we obtained was $\text{TS} = -0.54$. In order to assess the significance of this result, we computed TS for 10^6 Monte Carlo (MC) datasets generated assuming an isotropic flux, and found $\text{TS} \geq -0.54$ in $p = 12.3\%$ of the 10^6 cases, corresponding to a 1.2σ significance.²

We also computed test statistics for 10^6 MC sets generated under an assumption of the Auger best-fit SBG flux model to know the range of TS values that could be expected in that case. The results are shown in Figure 2. We found that 90.9% of realizations in the latter case

have a higher TS value than the TA data (corresponding to a -1.3σ significance). We also verified that, as should be by design, the ratio between the two TS distributions is $\exp(\text{TS}/2)$. A negative TS means that the angular distribution in a dataset resembles isotropy more than the SBG model, and a positive TS means the reverse, so most isotropic realizations have $\text{TS} < 0$ and most SBG-like realizations have $\text{TS} > 0$. $\text{TS} \approx 0$ would mean that the angular distribution in a dataset is about equally different from the two models considered.

4. DISCUSSION

A limitation in this analysis is the exclusion of Local Group objects (SMC, LMC, M33 and M31), which were listed in Ackermann et al. (2012), but in a separate table. These objects are not particularly intrinsically luminous (several times less than the dimmest objects in Table 1), but due to their proximity ($D = 0.06, 0.05, 0.85$ and 0.78 Mpc respectively) they appear very bright. If the assumed proportionality between the UHECR luminosity, the star-formation rate and the radio luminosity also applied to them, then the LMC and SMC would outshine all other objects combined in the Auger sky, and M33 and M31 would be the second and third brightest objects in the TA sky; but no excess of events is apparent in the vicinity of either pair of objects in our data or in Aab et al. (2018). A discussion about possible theoretical astrophysical motivations for not including these objects in the sample is outside the scope of this work.

Aab et al. (2018) also tested their data for correlations with gamma-ray loud AGNs from the 2FHL catalog (Ackermann et al. 2016). The best fit ($E_{\text{min}} = 60$ EeV, $f_{\gamma\text{AGN}} = 6.7\%$, $\theta = 6.9^\circ$) is favored over isotropy at the 2.7σ level. Unlike with SBGs, UHECR energy losses in propagation are not negligible in this case because the unattenuated flux is not dominated by nearby objects. Testing TA data for correlations with this catalog would not be very useful, because the attenuated flux at Earth is dominated by Cen A, way outside the TA field of view (at $\delta = -43^\circ$), leaving the flux in the northern hemisphere very nearly isotropic, and therefore requiring a very large number of events for an experiment in the northern hemisphere to detect the correlation; also, the Auger best-fit energy threshold found with this catalog ($E_{\text{min}} = 60$ EeV) was higher than with the SBGs, further reducing the available statistics.

5. CONCLUSIONS

This Letter presents the result of a search for a correlation between arrival directions of UHECRs observed by TA and the flux pattern of SBGs. The SBG sample, anisotropic fraction and angular scale were fixed

² Note that unlike in the Auger analysis, Wilks' theorem is not applicable here because we did not scan a parameter space which the null hypothesis is a subspace of.

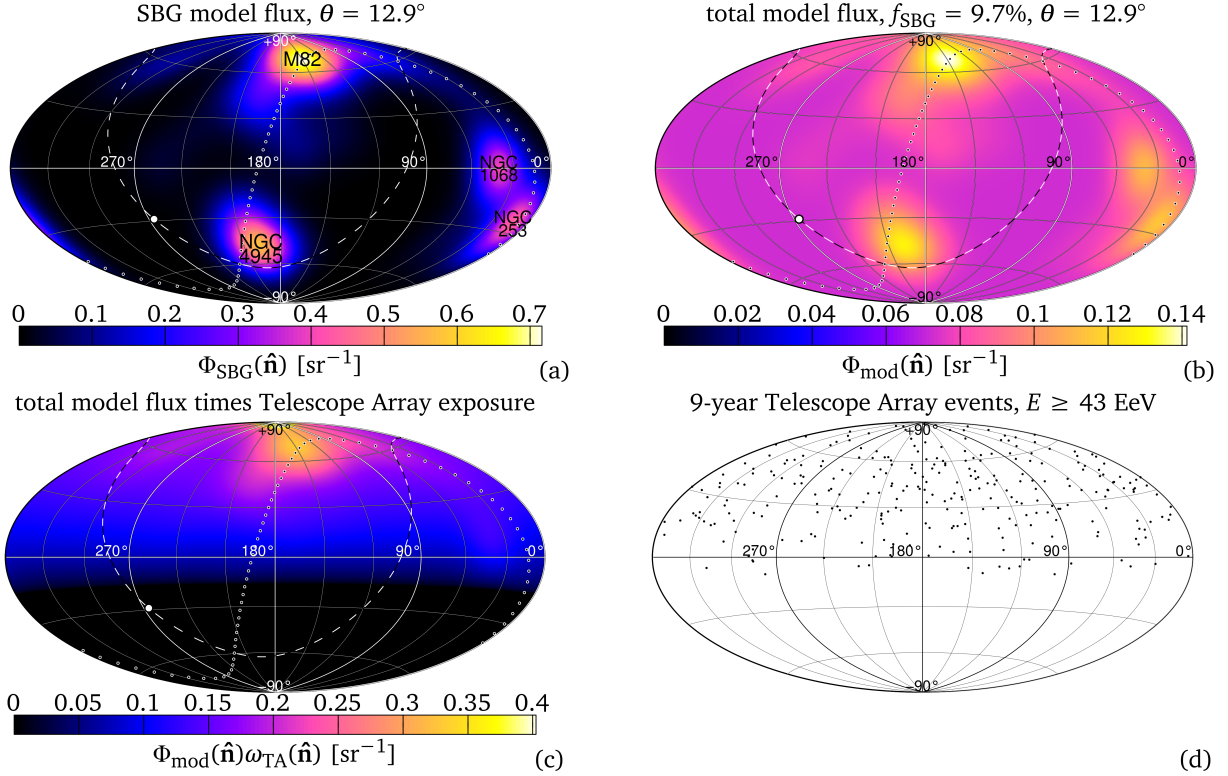


Figure 1. Maps of: (a) the anisotropic part of the model flux (equation 4); (b) the total model flux (equation 3); (c) the total model flux multiplied by the TA exposure; and (d) the TA events above 43 EeV. The dashed and dotted lines represent the Galactic and supergalactic planes respectively and the white disk shows the Galactic center.

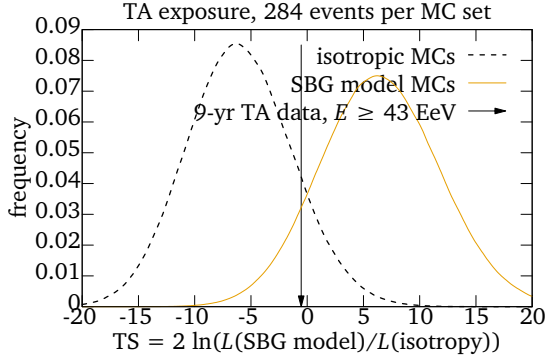


Figure 2. Distribution of test statistics in MC sets generated according to the two flux hypotheses we considered.

to be the best-fit values as in the Auger study. The energy threshold of 43 EeV was determined by taking into account of the energy scale difference between two experiments (AbuZayyad et al. 2018), corresponding to 39 EeV at which the most significant correlation was reported in Auger. The result of this test was inconclusive, being compatible both with isotropy to within 1.2σ and with the Auger result to within 1.3σ . The ongoing expansion of TA (Kido 2018) will increase its effective area by a factor of 4, allowing us to reduce the statis-

tical uncertainties and possibly to discriminate between different hypothesis about the UHECR origin.

ACKNOWLEDGMENTS

We thank Pierre Auger collaboration members Jonathan Biteau and Olivier Deligny for useful discussions about their analysis.

The Telescope Array experiment is supported by the Japan Society for the Promotion of Science (JSPS) through Grants-in-Aid for Priority Area 431, for Specially Promoted Research JP21000002, for Scientific Research (S) JP19104006, for Specially Promoted Research JP15H05693, for Scientific Research (S) JP15H05741 and for Young Scientists (A) JPH26707011; by the joint research program of the Institute for Cosmic Ray Research (ICRR), The University of Tokyo; by the U.S. National Science Foundation awards PHY-0601915, PHY-1404495, PHY-1404502, and PHY-1607727; by the National Research Foundation of Korea (2016R1A2B4014967, 2016R1A5A1013277, 2017K1A4A3015188, 2017R1A2A1A05071429); by the Russian Academy of Sciences, RFBR grant 16-02-00962a (INR), IISN project No. 4.4502.13, and Belgian Science Policy under IUAP VII/37 (ULB). The foundations of Dr. Ezekiel R. and Edna Wattis Dumke, Willard L. Eccles, and George S. and Dolores Doré Eccles all helped with generous dona-

tions. The State of Utah supported the project through its Economic Development Board, and the University of Utah through the Office of the Vice President for Research. The experimental site became available through the cooperation of the Utah School and Institutional Trust Lands Administration (SITLA), U.S. Bureau of Land Management (BLM), and the U.S. Air Force. We appreciate the assistance of the State of Utah and Fillmore offices of the BLM in crafting the Plan of Development for the site. Patrick Shea assisted the collaboration with valuable advice on a variety of topics.

The people and the officials of Millard County, Utah have been a source of steadfast and warm support for our work which we greatly appreciate. We are indebted to the Millard County Road Department for their efforts to maintain and clear the roads which get us to our sites. We gratefully acknowledge the contribution from the technical staffs of our home institutions. An allocation of computer time from the Center for High Performance Computing at the University of Utah is gratefully acknowledged.

REFERENCES

- Aab, A., et al. 2015, *Nucl. Instrum. Meth.*, A798, 172, doi: [10.1016/j.nima.2015.06.058](https://doi.org/10.1016/j.nima.2015.06.058)
- . 2018, *Astrophys. J.*, 853, L29, doi: [10.3847/2041-8213/aaa66d](https://doi.org/10.3847/2041-8213/aaa66d)
- Abbasi, R. U., et al. 2014, *Astrophys. J.*, 790, L21, doi: [10.1088/2041-8205/790/2/L21](https://doi.org/10.1088/2041-8205/790/2/L21)
- . 2016, *Astropart. Phys.*, 80, 131, doi: [10.1016/j.astropartphys.2016.04.002](https://doi.org/10.1016/j.astropartphys.2016.04.002)
- Abu-Zayyad, T., et al. 2013a, *Nucl. Instrum. Meth.*, A689, 87, doi: [10.1016/j.nima.2012.05.079](https://doi.org/10.1016/j.nima.2012.05.079)
- . 2013b, *Astrophys. J.*, 768, L1, doi: [10.1088/2041-8205/768/1/L1](https://doi.org/10.1088/2041-8205/768/1/L1)
- AbuZayyad, T., et al. 2018, *JPS Conf. Proc.*, 19, 011003, doi: [10.7566/JPSCP.19.011003](https://doi.org/10.7566/JPSCP.19.011003)
- Ackermann, M., et al. 2012, *Astrophys. J.*, 755, 164, doi: [10.1088/0004-637X/755/2/164](https://doi.org/10.1088/0004-637X/755/2/164)
- . 2016, *Astrophys. J. Suppl.*, 222, 5, doi: [10.3847/0067-0049/222/1/5](https://doi.org/10.3847/0067-0049/222/1/5)
- Kido, E. 2018, *JPS Conf. Proc.*, 19, 011025, doi: [10.7566/JPSCP.19.011025](https://doi.org/10.7566/JPSCP.19.011025)
- Sommers, P. 2001, *Astropart. Phys.*, 14, 271, doi: [10.1016/S0927-6505\(00\)00130-4](https://doi.org/10.1016/S0927-6505(00)00130-4)
- Tokuno, H., et al. 2012, *Nucl. Instrum. Meth.*, A676, 54, doi: [10.1016/j.nima.2012.02.044](https://doi.org/10.1016/j.nima.2012.02.044)
- Tsunesada, Y., AbuZayyad, T., Ivanov, D., et al. 2017, *PoS, ICRC2017*, 535
- Verzi, V., Ivanov, D., & Tsunesada, Y. 2017, *PTEP*, 2017, 12A103, doi: [10.1093/ptep/ptx082](https://doi.org/10.1093/ptep/ptx082)